The Study of The Contact Between the Wheel and The Track in The Case of a Vehicle Equipped with A Semi-Active Suspension

Dinel POPA *
National University of Science and Technology Politehnica Bucharest, University center of Piteşti, street Tg. din Vale, no. 1, dinel_popa@yahoo.com

Nicoleta OLĂRESCU
National University of Science and Technology Politehnica Bucharest, University center of Piteşti, street Tg. din Vale, no. 1, nicoletadim4@yahoo.com

Claudia-Mari POPA
National University of Science and Technology Politehnica Bucharest, University center of Piteşti, street Tg. din Vale, no. 1, claudia_mari_1965@yahoo.com

* Author to whom correspondence should be addressed

Abstract: - The paper presents a dynamic model with 4 degrees of freedom that allows the study of pitch and swing bounce vibrations for independent suspensions. Based on this model and the results obtained, an electronic control system of a semi-active suspension can be achieved. The displacement equations obtained by applying the theorem of the center of mass and the kinetic moment are presented in matrix form. Based on this information, the influence of travel speed and the value of damping constants of the suspension shock absorbers on the amplification factors of displacement amplitudes and dynamic forces at the two wheels is studied. At the end of the paper, the results obtained on a numerical application with the data of a medium class car are presented and interpreted.

Keywords: - suspension, dynamic model, displacement equations, harmonic excitations, random excitations

1. INTRODUCTION

During the movement of a vehicle, translational (jerking, skidding and bouncing) and rotational (rolling or rocking, pitching and yawing) vibrations are produced and transmitted from the road to the passengers. These vibrations affect the human body (comfort sensation) and the normal reactions at the wheels [1].

By imprinting the desired character of the oscillations, the suspension, together with the steering mechanism of the wheels, influences the handling, maneuverability and stability of the car, elements that together define the road holding of the vehicle [2].

Suspension, based on elastic and damping characteristics, can be: passive, semi-active and active. A passive suspension system is a system in which the coefficients of the components of which it is made up remain constant, a semi-active suspension system is developed from the passive system in which the damping characteristic can change, in a controlled manner, depending on the conditions of use of the vehicle, and an active suspension is also developed from a passive suspension where in addition there is a force actuator that controls the elastic and damping characteristics [3]. So, by definition, a suspension is active if certain parameters of it can change during functioning [4],[6]. Due to the high costs of component active shock absorbers, sensors, electronic vehicle control unit, etc., this type of suspension has not been widely adopted.

Fitting an F1 car by Lotus engineers more than 30 years ago with an active suspension was not a success mainly due to the additional energy consumption, additional vibration introduction and high manufacturing costs for the components.

Over time, the weaknesses were remedied by the engineering departments of the major car manufacturers: Mercedes-Benz, BMV, Opel, Toyota, Volkswagen, Citroen, etc. [8]. Today, thanks to the falling prices of active suspension elements, manufacturers equip their luxury models with this type of suspension, each developing its own system: Toyota and Lexus developed the AVS system, BMV uses the Adaptive Drive system, Porsche uses the active PASM system, Opel DSS continuous damping system, Mercedes-Benz ADS adaptive damping system [9].

The electronic command and control systems of an active suspension are based on algorithms resulted from the notions of dynamic systems theory [1]. A dynamic system is a set of elements that communicate with each other. The basis of this assembly is a dynamic model for which a controller is designed that

evaluates first the variables to be controlled, then the feedback is compared with the reference point [5],[7].

Dynamic models used in the study of semi-active and active suspensions are usually with 2 degrees of freedom [4]. The paper presents a model with 4 degrees of freedom, a model that allows obtaining results close to models with a larger number of degrees of freedom [10],[11]. The models with several degrees of freedom allow obtaining numerical results also regarding the vibrations on the passenger seats [1].

2. DYNAMIC MODEL WITH 4 DEGREES OF FREEDOM

2.1. Dynamic model

The model in Figure 1 can be used for the analysis of pitch bounce vibrations and rock bounce vibrations in the case of independent suspensions. In the literature it is also known as a half car model. The suspension elements in Figure 1 are represented in the equilibrium position, on a bumpy road.

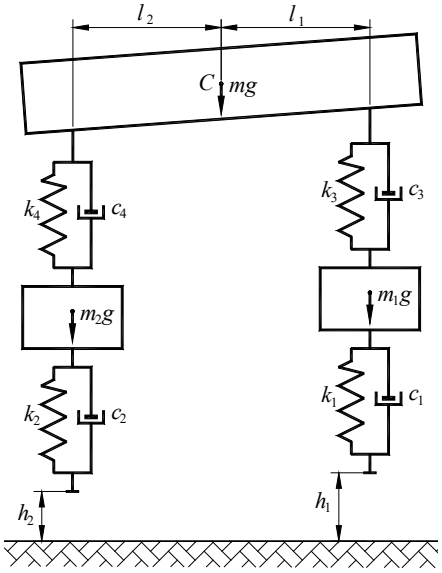

Figure 1. Model with four degrees of freedom.

The notations used were: C - the center of gravity of the suspended mass, m_1, m_2 - the equivalent mass of the wheels, m - suspended mass, h_1, h_2 - roadway bumps, k_1, k_2 - the elastic constants of the tires, c_1, c_2 - tire damping constants, c_3, c_4 - the damping constants of the shock absorbers, k_3, k_4 - the elastic constants of the springs, l_1, l_2 - the distances of center of gravity from the wheel axis.

2.2. Static forces at the wheels

Figure 2 shows the isolated elements in static equilibrium. Using notations: z_{10}, z_{20} - the static arrows of the tires, z_{30}, z_{40} - the static arrows of the springs, $l = l_1 + l_2$ - the distance between the wheels, from the equilibrium equations, we obtain the static arrow expressions:

$$z_{10} = \frac{g(m_1 l + m l_2)}{k_1 l},\ z_{20} = \frac{g(m_2 l + m l_1)}{k_2 l},$$
$$z_{30} = \frac{g(m l_2)}{k_3 l},\ z_{40} = \frac{g}{k_4 l}(m l_1) \qquad (1)$$

and of the static forces at the two wheels:

$$F_{1S} = g\left(m_1 + \frac{l_2}{l}m\right),\ F_{2S} = g\left(m_2 + \frac{l_1}{l}m\right). \qquad (2)$$

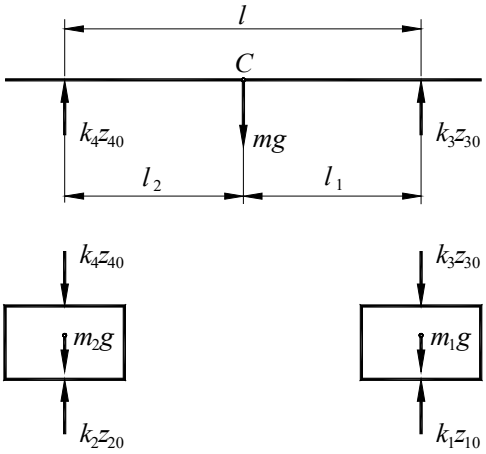

Figure 2. Static equilibrium of suspension elements.

2.3. The forces that act during the movement

Figure 3 shows the car suspension elements in dynamic balance.

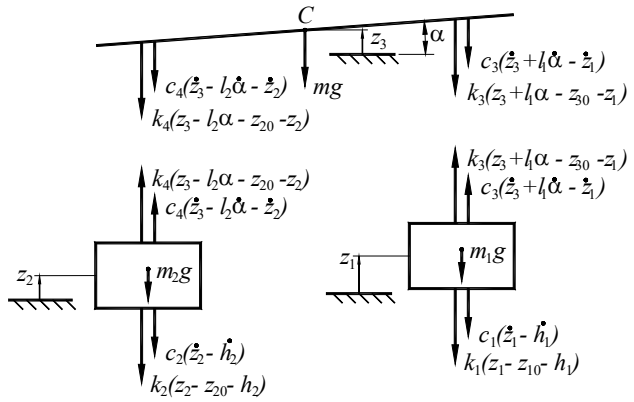

Figure 3. The dynamic equilibrium of the suspension elements.

For the suspended mass m were considered the displacements: z_3 - the displacement of the center of gravity relative to the equilibrium position, α - the angle of inclination from the equilibrium position. For wheel masses m_1, m_2 were considered the

displacements: z_1, z_2, - displacements measured from the equilibrium position.

2.4. Displacement equations

In order to obtain the displacement equations, the theorem of the movement of the center of mass is applied for all elements and the theorem of the kinetic moment for the suspended mass. Using notation J_C for the moment of inertia of the suspended mass, we obtain the following equations in matrix form:

$$[M]\{\ddot{Z}\}+[C]\{\dot{Z}\}+[K]\{Z\}=\{F\}. \quad (3)$$

The established notations were used, where: $[M]$ is the mass matrix (of inertia), $[C]$ is the viscous damping matrix, $[K]$ is the stiffness matrix, $\{Z\}$ is the column matrix of the parameters that define the movement, and $\{F\}$ is the column matrix of excitations. The matrix expressions are:

$$[M]=\begin{bmatrix} m_1 & 0 & 0 & 0 \\ 0 & m_2 & 0 & 0 \\ 0 & 0 & m & 0 \\ 0 & 0 & 0 & J_C \end{bmatrix}, \quad (4)$$

$$[C]=\begin{bmatrix} c_1+c_3 & 0 & -c_3 & -c_3l_1 \\ 0 & c_2+c_4 & -c_4 & c_4l_2 \\ -c_3 & -c_4 & c_3+c_4 & c_3l_1-c_4l_2 \\ -c_3l_1 & c_4l_2 & c_3l_1-c_4l_2 & c_3l_1^2+c_4l_2^2 \end{bmatrix}, \quad (5)$$

$$[K]=\begin{bmatrix} k_1+k_3 & 0 & -k_3 & -k_3l_1 \\ 0 & k_2+k_4 & -k_4 & k_4l_2 \\ -k_3 & -k_4 & k_3+k_4 & k_3l_1-k_4l_2 \\ -k_3l_1 & k_4l_2 & k_3l_1-k_4l_2 & k_3l_1^2+k_4l_2^2 \end{bmatrix}, \quad (6)$$

$$\{F\}=\begin{pmatrix} k_1h_1+c_1\dot{h}_1 & k_2h_2+c_2\dot{h}_2 & 0 & 0 \end{pmatrix}^T. \quad (7)$$

The column matrix of the parameters that define the movement is:

$$\{Z\}=\begin{pmatrix} z_1 & z_2 & z & \alpha \end{pmatrix}^T. \quad (8)$$

As excitations h_1 and h_2 are time dependent:

$$h_1=h_1(t),\ h_2=h_2(t-t_0) \quad (9)$$

and excitation forces:

$$F_1=k_1h_1+c_1\dot{h}_1,\ F_2=k_2h_2+c_2\dot{h}_2 \quad (10)$$

they are also time dependent.

Noting with v the speed of the car, in the case of pitch bounce vibrations, the time lag t_0 is given by the relation:

$$t_0=\frac{l}{v}. \quad (11)$$

The model with 4 degrees of freedom presented can be used in the case of the study of bouncing - pitching vibrations, but also in the study of bouncing - rocking vibrations.

In the case of *the bounce-pitch vibration study,* the car moves with speed v, mass m_1 from Figure1 being the mass of the front wheel and m_2 is the mass of the rear wheel. In this case, the distances l_1 and l_2 define the longitudinal position of the center of gravity of the suspended mass, and the distance l defines the distance between the front and rear wheels.

In the case of *the bounce-rocking vibration study*, m_1 and m_2 are the masses of the wheels from an axle with independent suspension. The distances l_1 and l_2 define the transverse position of the center of gravity of the suspended mass ($l_1=l_2$), and the distance l defines the distance between the wheels on the same axle. The speed v from Figure1 is in a direction perpendicular to the plane of the figure, and the time lag $t_0=0$.

2.5. Vertical dynamic forces at the wheels

The vertical dynamic forces at the wheels have two components: static and dynamic. The static forces are given by the relations (2), and the dynamic forces are given by the expressions:

$$F_{1D}=-k_1(z_1-h_1)-c_1(\dot{z}_1-\dot{h}_1),$$
$$F_{2D}=-k_2(z_2-h_2)-c_2(\dot{z}_2-\dot{h}_2). \quad (12)$$

Taking these considerations into account, the expressions of the vertical dynamic forces at the two wheels, F_{1R} and F_{2R}, are:

$$F_{1R}=F_{1S}+F_{1D},\ F_{2R}=F_{2S}+F_{2D}. \quad (13)$$

2.6. Natural pulsation and modal matrix

The natural pulsations are determined from the matrix equation:

$$[M]\{\ddot{Z}\}+[K]\{Z\}=\{0\}. \quad (14)$$

Own pulsation p_1, p_2, p_3, p_4 are determined by solving the characteristic equation:

$$\det[[K]-p^2[M]]=0. \quad (15)$$

The modal matrix is formed with the 4 own vectors $\{A_r\}$ on columns [1]:

$$[A]=[\{A_r(1)\}\ \{A_r(2)\}\ \{A_r(3)\}\ \{A_r(4)\}]. \quad (16)$$

2.7. Determination of the response to harmonic excitations

Road bumps can be considered to have a sinusoidal shape of amplitude h_0 and wavelength l. If the car is moving with speed v, then displacement x, based on time, is determined with relation $x=vt$

and time dependent function for bumps h has the expression:

$$h = h_0 \sin \omega t = h_0 \cos\left(\omega t - \frac{\pi}{2}\right), \quad (17)$$

where:

$$\omega = \frac{2\pi v}{l}. \quad (18)$$

Excitation function f has in this case the expression:

$$f = \frac{\omega}{2\pi} = \frac{v}{l}. \quad (19)$$

In the case of a motor vehicle, of interest are the intervals [1]:

$f \in [0{,}5 \ldots 25]$Hz for the excitation function,

$l \in [0{,}3 \ldots 100]$m for wavelengths,

$v \in [10 \ldots 50]$m/s for speeds.

Time lag t_0 between the front and rear wheels, if the vehicle is moving with constant speed v, the distance between the wheels being L, is:

$$t_0 = \frac{L}{v}. \quad (20)$$

The time function of the unevenness of the wheels on the same axle is:

$$h_j = h_{0j} \cos\left(\beta_j^0\right),\ j = 1{,}2, \quad (21)$$

and for wheels on different axles:

$$h_j = h_{0j} \cos\left(\omega t - \beta_j^0\right),\ j = 1{,}2. \quad (22)$$

The complex number method is used to calculate the response to harmonic excitations [1].

In real space, the following notations are used:

$$[TR] = [K] - \omega^2 [M], \quad (23)$$

$$[TC] = \omega [C]. \quad (24)$$

Based on them, the following can be determined:

- the transfer matrix $[\tilde{\eta}(\omega)]$ from forces to displacements, with the real component $[\tilde{\eta}R]$:

$$[\tilde{\eta}R] = \left[[TR] + [TC][TR]^{-1}[TC]\right]^{-1} \quad (25)$$

and complex component $[\tilde{\eta}C]$:

$$[\tilde{\eta}C] = -[TR]^{-1}[TC][\tilde{\eta}R], \quad (26)$$

- the transfer matrix $[\eta H(\omega)]$ from bumps to displacements, with the real component $[\eta HR]$:

$$[\eta HR] = [\tilde{\eta}R][KCR] - [\tilde{\eta}C][KCC] \quad (27)$$

and complex component $[\eta HC]$:

$$[\eta HC] = [\tilde{\eta}R][KCC] + [\tilde{\eta}C][KCR]. \quad (28)$$

The matrices $[KCR]$ and $[CCR]$ have different expressions for independent suspension and for rigid axle.

If the suspensions are independent, the following expressions are used:

$$[KCR] = \begin{bmatrix} k_1 & 0 & 0 & 0 \\ 0 & k_2 & 0 & 0 \\ 0 & 0 & k_3 & 0 \\ 0 & 0 & 0 & k_4 \end{bmatrix},$$

$$[KCC] = \begin{bmatrix} c_1\omega & 0 & 0 & 0 \\ 0 & c_2\omega & 0 & 0 \\ 0 & 0 & c_3\omega & 0 \\ 0 & 0 & 0 & c_4\omega \end{bmatrix}. \quad (29)$$

Next, using notations:

$$h_{jR} = h_{0j} \cos\beta_j^0,\ h_{jC} = -h_{0j} \sin\beta_j^0, \quad (30)$$

we obtain the vectors:

$$\{h_R\} = \begin{bmatrix} h_{1R} & h_{2R} & h_{3R} & h_{4R} \end{bmatrix}^T,$$

$$\{h_C\} = \begin{bmatrix} h_{1C} & h_{2C} & h_{3C} & h_{4C} \end{bmatrix}^T. \quad (31)$$

with which the two vectors of the stationary response are obtained:

$$\{Z_R^0\} = [\eta HR]\{h_R\} - [\eta HC]\{h_C\}, \quad (32)$$

$$\{Z_C^0\} = [\eta HR]\{h_C\} - [\eta HC]\{h_R\}. \quad (33)$$

With components Z_{jR}^0, Z_{jC}^0 the displacement amplitudes are obtained z_j:

$$Z_j^0 = \sqrt{\left(Z_{jR}^0\right)^2 + \left(Z_{jC}^0\right)^2}. \quad (34)$$

The dynamic forces from relations (12) have the expressions:

$$F_{jD}^* = \sqrt{\left(k_j^2 + \omega^2 c_j^2\right)} \cdot$$
$$\cdot \sqrt{\left(Z_{jR}^0 - h_{0j}\cos\beta_j\right)^2 + \left(Z_{jC}^0 + h_{0j}\sin\beta_j\right)^2}\,\cdot$$
$$j = 1,\ 2. \quad (35)$$

2.8. Determination of the response to random excitations

We consider the bumps for wheels on the same axle to be identical in shape and equal to $h(t)$ and respectively $\xi h(t)$. The power spectral density is also known $Sh(\omega)$.

In [1] expressions for the power spectral density are recommended:

$$Sh(\omega) = \begin{cases} \dfrac{2s_0\alpha v}{\omega^2 + \alpha^2 v^2} & \text{for } |\omega| < \omega_1 \\ 0 & \text{for } |\omega| > \omega_1 \end{cases}, \quad (36)$$

where $\omega_1 \le 10p$.

The matrix of the spectral density of wheel bumps $[SHR]$ has the components given in [1]. Based on them, the complex matrix of the spectral density of the response is determined:

$$[SZR]=[\eta HR][SHR][\eta HR]^T+[\eta HC][SHC][\eta HR]^T- \\ -[\eta HR][SHC][\eta HC]^T+[\eta HC][SHR][\eta HC]^T \quad (37)$$

$$[SZC]=[\eta HR][SHR][\eta HC]^T+[\eta HC][SHC][\eta HC]^T- \\ -[\eta HR][SHC][\eta HR]^T-[\eta HC][SHR][\eta HR]^T \quad (38)$$

Spectral power densities $S_{Zj}(\omega)$ are the elements located on the main diagonal of the matrix $[SZR]$. The effective values are thus obtained:

$$z_{jef}=\sqrt{\int_{-\omega_1}^{\omega_1}S_{Zj}(\omega)d\omega}\,. \quad (39)$$

For the spectral densities of the dynamic force at the wheels, the following are determined in order:
- interspectral density matrix $[S_{ZH}(\omega)]$ with components:

$$[S_{ZHR}]=[\eta HR][SHR]+[\eta HC][SHC], \quad (40)$$

$$[S_{ZHC}]=[\eta HR][SHC]-[\eta HC][SHR]. \quad (41)$$

- the power spectral density of the vertical forces at the wheels for wheels with independent suspensions:

$$S_{FjD}(\omega)=\left(k_j^2+c_j^2\omega^2\right)\left[S_{Zj}(\omega)-S_{Hj}(\omega)-2S_{ZjhjR}(\omega)\right]. \quad (42)$$

The effective values of the dynamic forces are:

$$F_{jDef}=\sqrt{\int_{-\omega_1}^{\omega_1}S_{FjD}(\omega)d\omega}\,. \quad (43)$$

3. NUMERICAL APPLICATION

In the case of this model, a numerical application was made for a car for which the following data are known: $m_1=32{,}5\,\text{kg}$ - the equivalent unsuspended mass of the front wheel, $m_2=26\,\text{kg}$ - the equivalent unsuspended mass of the rear wheel, $m=615\,\text{kg}$ – suspended mass, $J_C=850\,\text{kg}\cdot\text{m}^2$ - the moment of inertia with respect to the axis Cy, $l_1=1{,}05\,\text{m}$ - the distance of the center of gravity from the axis of the front wheel, $l_2=1{,}60\,\text{m}$ - center of gravity distance C to the rear wheel axle, $c_1=c_2=\dfrac{6000}{\omega}\,\text{Ns/m}$ - the damping constants of the front and rear tires, $k_1=k_2=120000\,\text{N/m}$ - the elastic constants of the front and rear tires, $k_3=22225\,\text{N/m}$ - the elastic constant of the front spring, $k_4=20067\,\text{N/m}$ - elastic constant of the rear spring, $v=10\,\text{m/s}$, $v=20\,\text{m/s}$ and $v=30\,\text{m/s}$ - 3 vehicle travel speeds, $Sh(\omega)=\dfrac{2s_0\alpha v}{\omega^2+\alpha^2v^2}$ - power density for paved roads, with the constants: $s_0=1{,}2\cdot10^4\ \text{m}^2$, $\alpha=0{,}45\ \text{m}^{-1}$.

The following will be determined: natural-pulsations, amplification factors of displacements and forces in the case of harmonic excitations, effective values of displacements and forces in the case of random excitations.

The numerical results are obtained with a calculation program in MATLAB language, program based on the calculation relations already established.

Numerical values are obtained for:
- wheels static arrows: $z_{10}=0{,}033\,\text{m}$, $z_{20}=0{,}022\,\text{m}$,
-spring static arrows: $z_{30}=0{,}1639\,\text{m}$, $z_{24}=0{,}1131\,\text{m}$,
- wheels static forces: $F_{1s}=3961{,}5\,\text{N}$, $F_{2s}=2645{,}6\,\text{N}$.

With relations $(14)\div(16)$ natural-pulsations and modal matrix are determined. The following numerical values for the natural frequencies are obtained:

$$f_1=1{,}1608\,\text{Hz},\ f_2=1{,}4326\,\text{Hz},\ f_3=10{,}5409\,\text{Hz},\ f_4=11{,}6902\,\text{Hz}$$

and modal matrix $[A]$ (natural vectors matrix):

$$[A]=\begin{bmatrix}0{,}204 & 0{,}065 & 0{,}999 & 0{,}000\\ 0{,}046 & -0{,}263 & 0{,}001 & -0{,}999\\ 0{,}906 & -0{,}469 & -0{,}008 & -0{,}006\\ 0{,}366 & 0{,}840 & -0{,}006 & -0{,}007\end{bmatrix}.$$

Analyzing the values obtained for the 4 vibration modes, the following can be concluded:
- vibration mode 1 (first natural vector): bounce vibrations of the suspended mass, moderate and in-phase vibrations for the front wheel and pitch vibrations of the suspended mass, negligible vibrations for the rear wheel;
- vibration mode 2: pitch vibrations for the suspended mass, moderate and in-phase vibrations for the rear wheel and for bouncing vibration of the suspended mass, negligible vibrations for the front wheel;
- vibration mode 3: vibration of the front wheel, insignificant vibrations of the other component parts;
- vibration mode 4: vibration of the rear wheel, insignificant vibrations of the other component parts.

To obtain values for displacement amplification factors, values are given to parameter ω in the range $(0\div155)\text{s}^{-1}$ with constant step $\Delta\omega=1$.

The influence of the travel speed and the influence of the damping constant of the shock absorber on the amplification factor of the displacement amplitudes are studied $\xi_1=\dfrac{z_1^0}{h_0}$, $\xi_2=\dfrac{z_2^0}{h_0}$, $\xi_3=\dfrac{z^0}{h_0}$, $\xi_4=\dfrac{\alpha^0}{h_0}$ given by relations (34) and the amplification factors of the dynamic forces F_{1D}, F_{2D} given by relations (35).

For an equal and constant value of the damping constants of the two dampers $c_1=c_2=c=1200\,\text{Ns/m}$ are considered 3 values of travel speed: $v=10\,\text{m/s}$, $20\,\text{m/s}$ and $30\,\text{m/s}$, and for a constant travel speed $v=30\,\text{m/s}$ are considered 3 values for damping

constants $c = 1000$ Ns/m, $c = 1500$ Ns/m and $c = 2000$ Ns/m.

Based on the values obtained with the calculation program, the graphs are drawn in figures 4 - 11 for the amplification factors of the displacement amplitudes ξ_1, ξ_2, ξ_3, ξ_4, based on travel speed $\xi_i(v)$ and based on damping constant value $\xi_i(c)$, as follows:

- in Figure 4, the graph of the amplification factor displays the amplitude of front wheel based on travel speed;

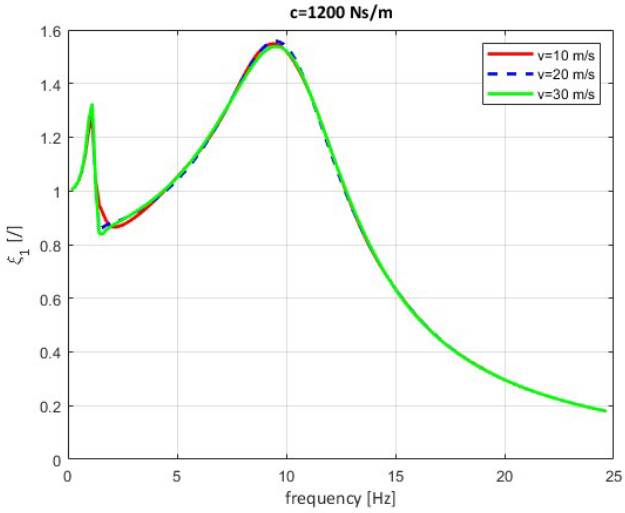

Figure 4. Amplification factor $\xi_1(v)$.

- in Figure 5, the graph of the amplification factor displays the amplitude of front wheel based on damping constant value;

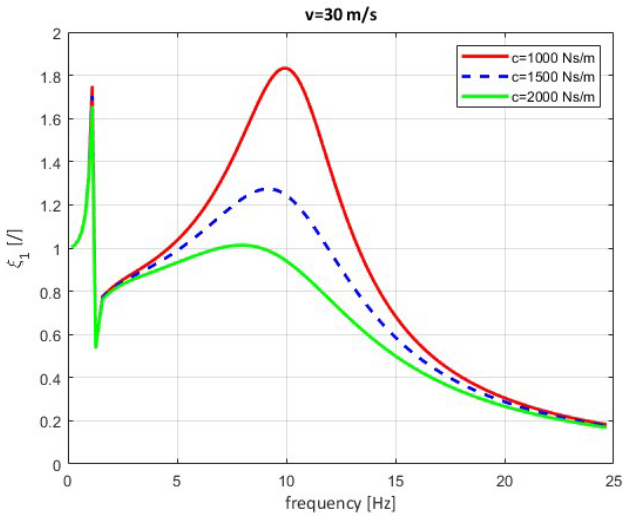

Figure 5. Amplification factor $\xi_1(c)$.

- in Figure 6, the graph of the amplification factor displays the amplitude of rear wheel based on travel speed;

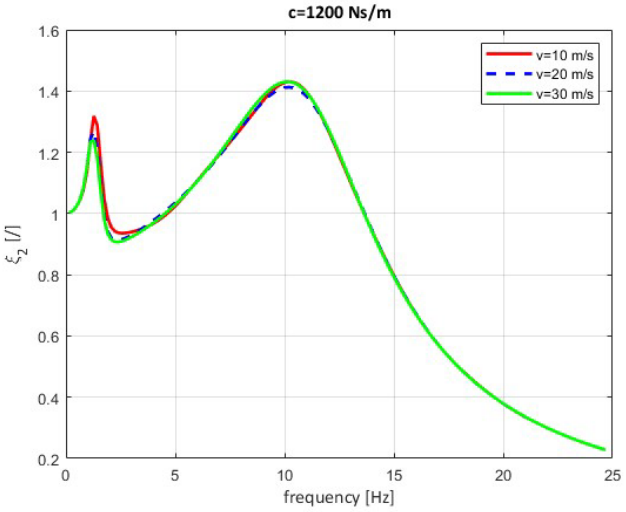

Figure 6. Amplification factor $\xi_2(v)$

- in Figure 7, the graph of the amplification factor displays the amplitude of rear wheel based on damping constant value;

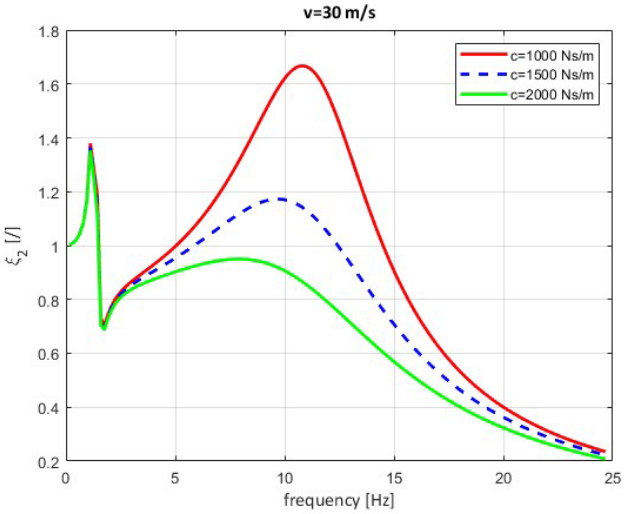

Figure 7. Amplification factor $\xi_2(c)$.

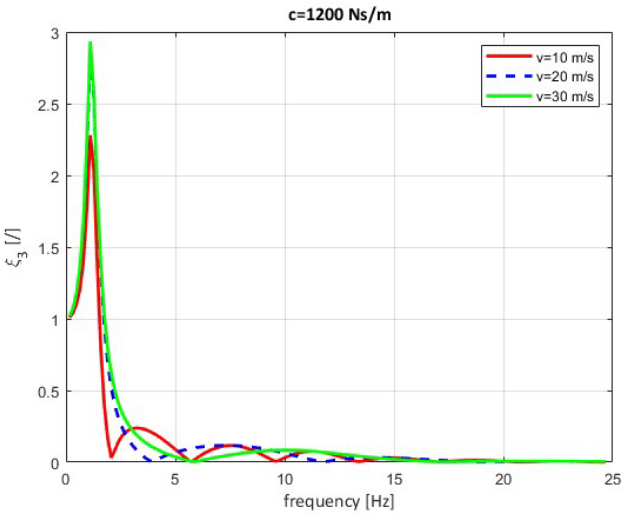

Figure 8. Amplification factor $\xi_3(v)$.

- in Figure 8, the graph of the amplification factor displays the amplitude of sprung mass based on travel speed;
- in Figure 9, the graph of the amplification factor displays the amplitude of sprung mass based on damping constant value;

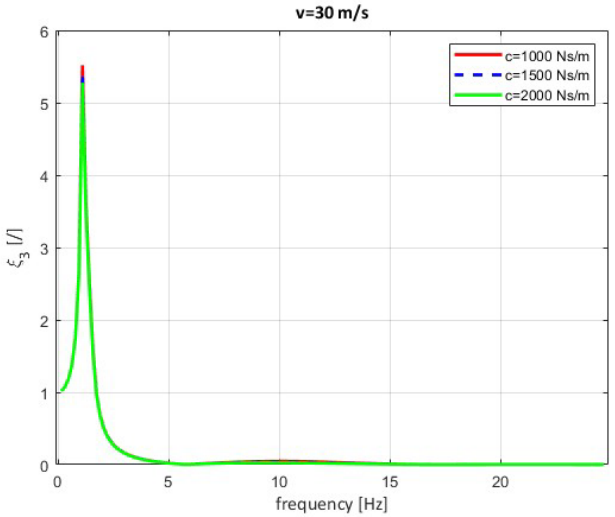

Figure 9. Amplification factor $\xi_3(c)$.

- in Figure 10, the graph of the amplification factor displays the amplitude of pitch angle based on travel speed;

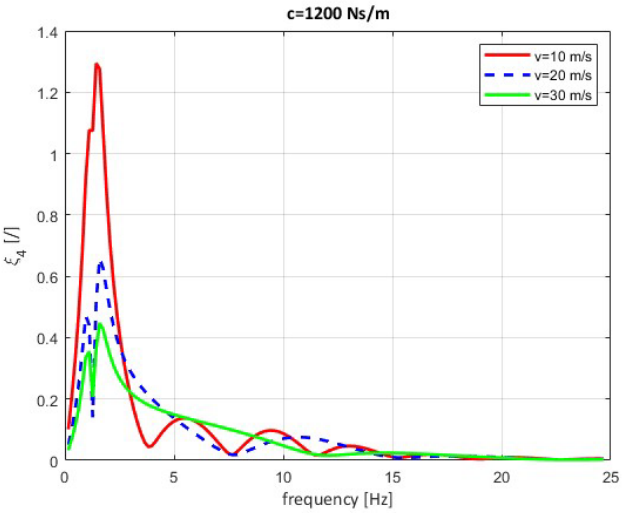

Figure 10. Amplification factor $\xi_4(v)$.

- in Figure 11, the graph of the amplification factor displays the amplitude of pitch angle based on damping constant value.

It is discovered that the displacement amplification factors $\xi_1(v)$, $\xi_2(v)$ are very little influenced by the speed of the vehicle, which is not the case for the displacement amplification factors $\xi_3(v)$ and $\xi_4(v)$.

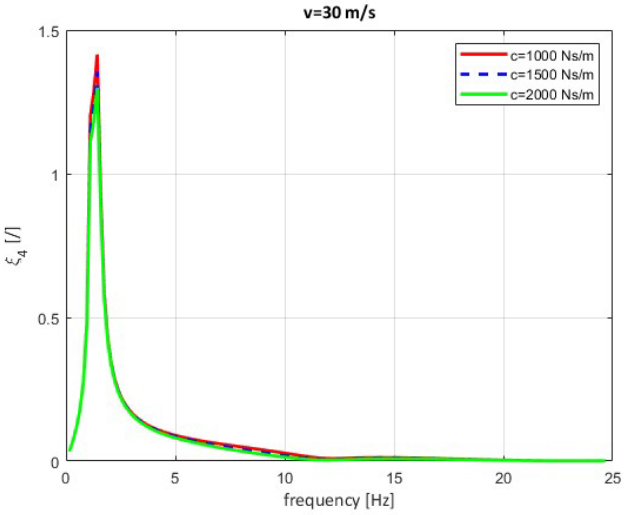

Figure 11. Amplification factor $\xi_4(c)$.

Instead, displacement amplification factors $\xi_1(c)$, $\xi_2(c)$ are strongly influenced by the value of the damping constant of the damper, thing that doesn't happen for displacement amplification factors $\xi_3(c)$ and $\xi_4(c)$.

For $c = 1200$ Ns/m, displacement amplification factors ξ_1, ξ_2 have a maximum at frequencies close to their own frequencies f_1, respectively f_2, followed by a level up to frequencies close to the own frequencies.

Proceeding in a similar way, the graphs of the amplification factors of the dynamic forces of the front and rear wheels are shown in the figures 12 to 15, as follows:

- in Figure 12, the graph of the amplification factor displays the amplitude of dynamic force of front wheel based on travel speed;

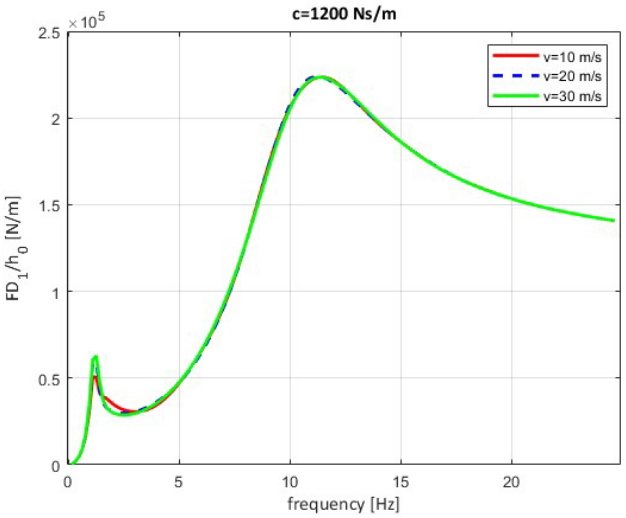

Figure 12. Amplification factor $FD_1(v)$.

- in Figure 13, the graph of the amplification factor displays the amplitude of dynamic force of front wheel based on damping constant value;

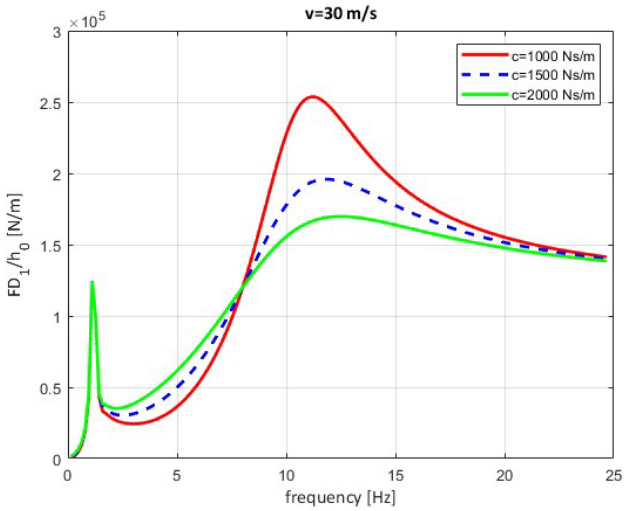

Figure 13. Amplification factor $FD_1(c)$.

- in Figure 14, the graph of the amplification factor displays the amplitude of dynamic force of rear wheel based on travel speed;

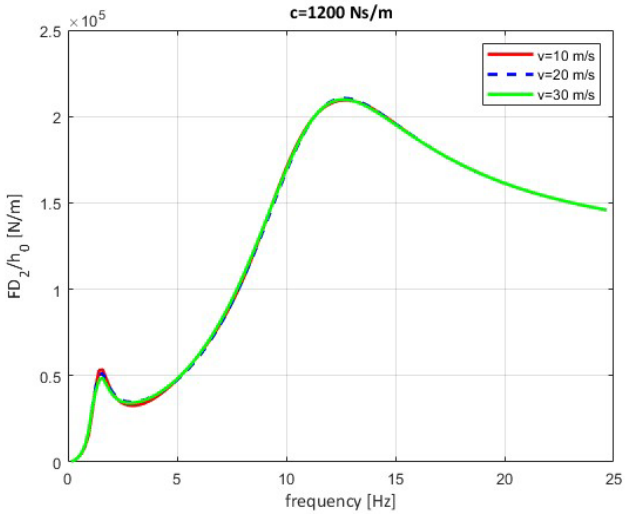

Figure 14. Amplification factor $FD_2(v)$.

- in Figure 15, the graph of the amplification factor displays the amplitude of dynamic force of rear wheel based on damping constant value.

Dynamic amplification factor $\frac{F_{1D}}{h_0}$ at front wheel has a maximum at the frequency close to the frequency f_1, the value being $\frac{F_{1D}}{h_0} = 223259 \frac{\text{N}}{\text{m}}$.

The static force at the front wheel being determined as $F_{1s} = 3961{,}5\,\text{N}$, it follows that for amplitudes h_0 higher than $\frac{3961{,}5}{223259} = 0{,}01777\,\text{m}$, meaning almost 18 mm, detachments occur at the front wheel.

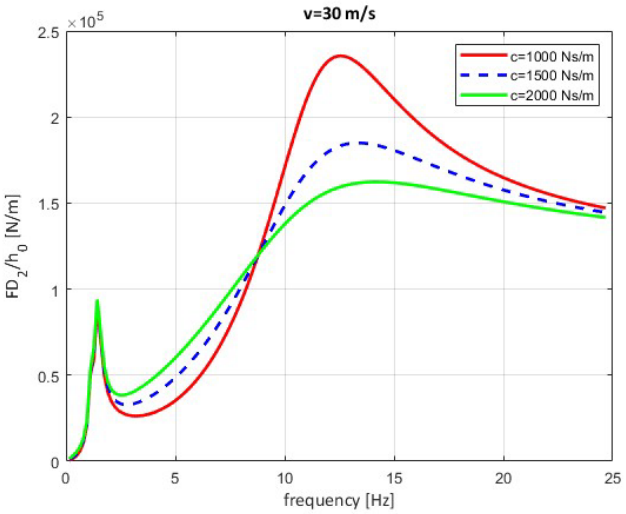

Figure 15. Amplification factor $FD_2(c)$.

The dynamic amplification factor $\frac{F_{2D}}{h_0}$ at rear wheel has a maximum at the frequency close to the frequency f_2, the value being $\frac{F_{2D}}{h_0} = 192512 \frac{\text{N}}{\text{m}}$. The static force at the rear wheel is $F_{2s} = 2645{,}6\,\text{N}$, so it follows that for amplitudes h_0 bigger than $\frac{2645{,}6}{192512} = 0{,}0137\,\text{m}$, meaning almost 14 mm, detachments occur at the rear wheel.

To determine the response of the system to random excitations, the calculation program continues. Considering the relations (36) ÷ (38), the components of the power spectral density matrices are calculated, with the help of which, the effective values of displacements z_{jef} are obtained, using relation (39).

The spectral densities of the dynamic force at the wheels are determined with the relations (40) and (42), and the effective value with (43).

From relations (39) are obtained the effective values of displacement z_{ief} depending on the 3 travel speed values in the Table 1.

Comparing the static values ($F_{1s} = 3961{,}5\,\text{N}$, $F_{2s} = 2645{,}6\,\text{N}$) with the dynamic ones, it can be concluded that on such a road (poorly cobbled) no separation occurs at the wheels for the 3 travel speeds considered.

Table 1.

Effective displacement values z_{jef} .

	z_{1ef} [mm]	z_{2ef} [mm]	z_{3ef} [mm]	z_{4ef} [rad]
v = 10 m/s,	25,4	25,1	23,8	0,0189
v = 15 m/s,	25,4	25,3	27,0	0,0159
v = 30 m/s,	25,1	25,2	26,1	0,0127

4. CONCLUSIONS

The contact between a car's wheel and the roadway is mainly influenced by the condition of the road, the value of the damping constant of the shock absorber and the travel speed.

In the case of an automobile, knowing a correspondence between these parameters leads to the possibility of designing a semi-active suspension that allows the damping factor to vary depending on the information received from the sensors that monitor the movements of the suspended and unsuspended masses.

With this information determined, a mechatronic system can be developed to control the activity of the damper.

This system uses the input information from the sensors and, with a software based on a control strategy, controls the mechatronic system that allows the damping constant to be changed. This ensures an optimal level of stability and comfort.

The dynamic model presented in the paper is with 4 degrees of freedom, and the application is performed for a car with independent suspensions for which a study of bounce-pitch vibrations is made.

For this model, also known in the literature as a half-car model, the influence of the car's travel speed and the values of the shock absorber's damping constant on the wheel-track contact is studied.

The study was carried out with the help of a calculation program in MATLAB, based on the calculation relations shown in this paper.

The calculation program allows obtaining the response of a dynamic system to harmonic excitations and random excitations, starting from the equations of motion, written in matrix form.

Using the matrix mode allows changes in the program for models with more degrees of freedom.

The applications were made for a medium class car for which were considered the travel speeds in the range of 10÷30 m/s and values of the damping constants in the range of 1000÷2000 Ns/m.

Comparing the obtained numerical results, it was observed that the values of the displacement amplification factors at the front and rear wheels are not influenced by the travel speed, but are strongly influenced by the value of the damping constant (the maximum values are around the natural frequencies, they increase with the decrease of the damping constant of the front and rear shock absorbers).

On the other hand, the amplification factors of the suspended mass and the pitch angle are influenced only by the movement speed, the maximum being around the own frequencies of the suspended mass.

Likewise, the dynamic factors at the front and rear wheels are also influenced by the value of the damping constant.

The maximum values of the dynamic forces, in comparison with the static values, allows the determination of the maximum values of the displacements of the separation of the wheels from the track, depending on the value of the damping statement.

As a result of the study carried out for the analysis of the system's response to random excitations, the values of the spectral densities of the dynamic force at the wheels and the effective values of the displacements according to the three values of the considered displacement speed were obtained.

From the analysis of the values obtained, it was determined that, on a poorly paved road, the wheels do not loose contact with the roadway, for the considered speed values.

REFERENCES

[1] Pandrea, N., Popa D., Parlac S, *Modele Pentru Studiul Vibratiilor Automobilelor* , Ed. Tiparg, Pitesti, 2001.

[2] Untaru M, Poțincu G, Tabacu I, Stoicescu A and Pereș G, *Dinamica autovehiculelor pe roți,* Editura Didactică și Pedagogică, București, 1981.

[3] *Automotive Suspension & Steering Systems* 4th Edition, 2007.

[4] Giua A., Seatzu C., Usai G., *Semiactice Suspension Design with an Optimal Gain Switching Target Vehicle System Dynamics, International Journal of Vehicle Mechanics and Mobility* ,2011.

[5] Gervasi G., *Variable Stiffness Mechanical Leaf Spring Suspension and A Method for Adjusting Such Stiffness*, EP1541392-B1 Patent 2010.

[6] Guglielmino E., Sireteanu T., Stammers C., Ghita G., Giuclea M., Casey T., *Semi-active Suspension Control,* Springer-Verlag London Limited, 2008.

[7] Bourmistrova A., Storey I., Subic A., *Multiobjective Optimisation Of Active And Semi-Active Suspension Systems With Application Of Evolutionary Algorithm, In Modsim,* 16th Congress Of The Modelling And Simulation Society Of Australia And New Zealand, 2005.

[8] AMA Soliman, MMS Kaldas, Semi-active suspension systems from research to mass-market – A review, Journal of Low Frequency Noise, Vibration and Active Control, 2019.

[9] https://en.wikipedia.org/wiki/Active_suspension.

[10] Duc Ngoc Nguyen,Tuan Anh Nguyen, The Dynamic Model and Control Algorithm for the Active Suspension System, 2023.

[11] Tameshwer Nath, Vikas Rastogi, Dynamic Modeling and Simulation of Automotive Suspension System with Overwhelming Controller, ResearchGate, 2020.